PI3 kinase signaling is involved in Aβ-induced memory loss in *Drosophila*

Hsueh-Cheng Chiang[a,b,1], Lei Wang[c,1], Zuolei Xie[d], Alice Yau[a], and Yi Zhong[a,c,2]

[a]Cold Spring Harbor Laboratory, Cold Spring Harbor, NY 11724; [b]Department of Neuroscience, State University of New York, Stony Brook, NY 11794; [c]Department of Biological Sciences and Biotechnology, Tsinghua University, Beijing 100084, China; and [d]JoeKai, Inc., Beijing 100084, China

Edited by Yuh-Nung Jan, Howard Hughes Medical Institute, San Francisco, CA, and approved March 4, 2010 (received for review August 15, 2009)

Multiple intracellular signals are altered in Alzheimer's disease brain tissues, including the PI3K/Akt pathway. However, the pathological relevance of such alterations is poorly understood. In vitro studies yield results that seem to be consistent with the conventional perception in which an up-regulation of the cell survival pathway, PI3K pathway, is protective in Alzheimer's disease pathogenesis. The current in vivo genetic approach, however, reveals that inhibition of the PI3K pathway leads to rescuing of the β-amyloid peptide (Aβ)-induced memory loss in the *Drosophila* brain. We began our inquiry into the molecular basis of this memory loss by studying Aβ42-induced enhancement of long-term depression. We found that long-term depression is restored to a normal level through inhibition of PI3K activity. Aβ42-induced PI3K hyperactivity is directly confirmed by immunostaining of the PI3K phosphorylation targets, phospholipids. Such observations lead to the following demonstration that Aβ42-induced memory loss can be rescued through genetic silencing or pharmacological inhibition of PI3K functions. Our data suggest that Aβ42 stimulates PI3K, which in turn causes memory loss in association with an increase in accumulation of Aβ42 aggregates.

β-amyloid | Alzheimer's disease | learning and memory | PI3K

Two major clinical symptoms of Alzheimer's disease (AD) include early memory loss and massive late-onset neurodegeneration. Genetic studies of the early onset familial AD provide a causative link between AD and beta-amyloid (Aβ) peptides that are derived from a proteolytic cleavage of the amyloid precursor protein (APP) (1–3). A body of evidence suggests that Aβ peptides are capable of modifying a number of biochemical pathways, such as PI3K, C-Junk, caspase, cyclin-dependent kinase 5 (cdk5), and others (4, 5). An alteration in these pathways may lead to a wide range of cellular dysfunctions, such as disturbed metal ion homeostasis, Ca^{2+} dysregulation, and impaired neurotransmission. However, how Aβ42 alters these signaling pathways is still unclear. Furthermore, because most of these studies are performed in in vitro or semi in vivo preparations, the relevance of any of these alterations to pathological phenotypes is not well-studied.

We sought to gain insights into the biochemical processes that mediate the Aβ toxicity through in vivo study of Aβ42-transgenic fruit flies. Expression of human APP or Aβ in the *Drosophila* brain recapitulates many features of AD (6). Our previous study has shown that expression of a secretory form of Aβ42 in the fly brain could induce age-dependent memory loss, massive neurodegeneration, accumulation of Aβ42 oligomers, and fibril deposits (7, 8). Because the APP family proteins and Aβ42 produce similar pathologic phenotypes across a wide range of organisms from invertebrates to mammals, the molecular basis of Aβ42 toxicity is likely conserved (9–12). An APP-like (APPL) *Drosophila* protein has been reported to give rise to a cleaved peptide capable of forming amyloidogenic deposits and causing neurodegeneration (11).

This study focuses on the biochemical pathways through which Aβ42 induces an age-dependent memory loss. An earlier study reported that Aβ42 alters long-term depression (LTD) at the larval neuromuscular junction (NMJ) (13). In *Drosophila*, this preparation is the only one suitable for quantitative analysis of synaptic transmission at identified synapses (14, 15). Although LTD at the NMJ is not related with the memory formation, its underlying regulatory molecular mechanisms may share similar components, because many learning and memory mutants show altered synaptic plasticity at the NMJ (16). Indeed, the observations obtained at the NMJ led us to show that increased PI3K activity contributes to the Aβ42-induced memory loss, and this memory loss could be prevented through inhibition of PI3K activity.

Results

As indicated earlier, we wanted to begin our searching of molecular events underlying the Aβ42-induced memory loss from analysis of LTD. The two-electrode voltage-clamp method was used to investigate synaptic plasticity at the larval body wall NMJ, which has been extensively characterized (14, 15). Various forms of synaptic plasticity can be elicited at this glutamatergic synapse (16, 17), including short-term facilitation, posttetanic potentiation, and LTD. Although LTD in larval NMJ is mainly expressed at the presynaptic site, which is different from other preparations in which LTD is expressed at both pre- and postsynaptic sites, the properties of LTD are quite similar to those of vertebrate preparations (17). We have reported that LTD is strongly reduced in the *akt* mutants, but this defect can be rescued by acute expression of the normal *akt* transgene (17). Our previous work has shown that extracellular accumulation of Aβ42 aggregates leads to enhanced LTD (13), and this is shown again in the current study (Fig. 1*A*). The enhancement was mild but consistent and statistically significant. Because the observed LTD is known to be regulated by Akt (17), which is a downstream target of PI3K, we decided to investigate if Aβ42-induced LTD enhancement is related to the PI3K/Akt pathway.

With a tetanic stimulation, LTD was reliably elicited, and enhancement of LTD was evident in larvae with targeted expression of Aβ42 in muscle cells (*G7/+;UAS-Aβ42/+*) (Fig. 1*A*), presumably resulting from secretion of Aβ42 fibril aggregates (13). Aβ42 expression in presynaptic motor neurons has no observable effects on LTD, likely because of secretion of different forms of aggregates compared with muscle cells (13). Application of 25 nM wortmannin, a PI3K-specific inhibitor, to the NMJ reduced LTD to the control level in Aβ42-expressing larvae (Fig. 1*B*), suggesting that Aβ42-induced LTD enhancement resulted from elevated PI3K activity.

To verify this conclusion with more direct observations, we moved on to determine levels of PI3K phosphorylation targets,

Author contributions: H.-C.C., L.W., and Y.Z. designed research; H.-C.C., L.W., Z.X., and A.Y. performed research; H.-C.C. and L.W. contributed new reagents/analytic tools; H.-C.C., L.W., and Y.Z. analyzed data; and H.-C.C., L.W., and Y.Z. wrote the paper.

The authors declare no conflict of interest.

This article is a PNAS Direct Submission.

[1]H.-C.C. and L.W. contributed equally to this work.

[2]To whom correspondence should be addressed. E-mail: zhongyi@cshl.edu.

This article contains supporting information online at www.pnas.org/cgi/content/full/0909314107/DCSupplemental.

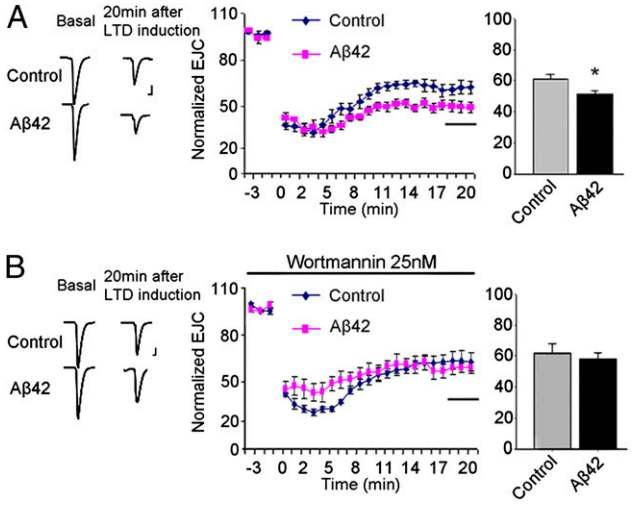

Fig. 1. Aβ42-enhanced LTD is reversed by application of the PI3K inhibitor at the NMJ. (*A* and *B*) Third-instar larvae were used for electrophysiology analysis. Evoked junctional currents (EJCs) were recorded in 0.4 mM Ca^{2+} saline. LTD was induced by tetanic stimulation of 30 Hz for 20 seconds. Representative EJCs traces (*Left*, scale is 10 nA vertical and 7.5 ms horizontal) for each genotype are normalized to the basal level before tetanic stimulation (*Center*). (*A Right*) LTD is enhanced after expression of Aβ42 driven by G7-Gal4 (*G7/+; UAS-Aβ42/+*) compared with control (*G7/+; +/+*) (means ± SEM; *t* test; $*P < 0.05$; $n = 5$). (*B Right*) Application of 25 nM wortmannin, the PI3K inhibitor, during test could reverse the Aβ42-induced LTD enhancement to the same level as the control (means ± SEM; $n = 6$).

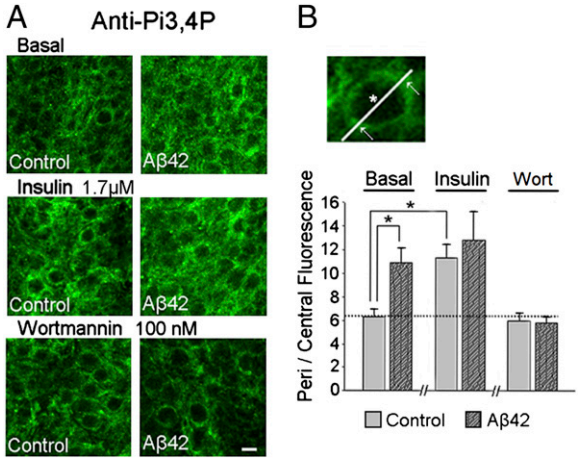

Fig. 2. Expression of Aβ42 increases the PI3,4P level through activation of the PI3K activity. (*A*) Larval ventral ganglion neurons from control (*elav/Y;+/+*) and Aβ42-expressing (*elav/Y;UAS-Aβ42/+*) flies were fixed and stained with anti-PI3,4P antibody without treatment (basal) or after 30 minutes of treatment with 1.7 μM insulin or 100 nM wortmannin (Wort), respectively. (*B Upper*) Single cells with strong fluorescence and well-defined boundaries were chosen for measuring the ratio of the plasma membrane fluorescence intensity (arrows) and the cytosolic fluorescence intensity (star). (*Lower*) The fluorescence ratio of each group of neurons is presented. The PI3,4P level was significantly increased in Aβ42-expressing neurons compared with control neurons without treatment (*t* test; $*P < 0.05$). This Aβ42-induced phenotype was reversed after wortmannin treatment. Incubation with insulin increased the Pi3,4P level in control neurons (*t* test; $*P < 0.05$) but not in Aβ42-expressing neurons compared with those without treatment. Data are expressed as means ± SEM ($n = 30$, 15, and 15 cells for nontreatment, insulin treatment, and wortmannin treatment, respectively). (Scale bar, 10 μm.)

phosphatidylinositol-3,4-bisphosphate (Pi3,4P) and phosphatidylinositol-3,4,5-trisphosphate (Pi3,4,5P), through immunostaining but in a larval ventral ganglion preparation. This preparation allowed a study of more general neuronal effects of Aβ42 instead of confining study to the NMJ. Moreover, this preparation is suitable for studying the effects of intended drug treatment (18, 19). Vertebrate insulin is known to activate *Drosophila* receptors of insulin-like peptides that are coupled to PI3K (20). We, therefore, incubated vertebrate insulin with isolated larval ventral ganglion and quantified the level of phospholipids using fluorescence intensity ratios obtained by immunostaining with specific antibodies (Fig. 2*A*). Single cells in the ganglion with strong fluorescence and well-defined boundaries were chosen for measuring the ratio of peripheral over central fluorescence intensities (Fig. 2*B Upper*). This ratio was used to reflect the phospholipid level and thereby, the PI3K activity. We found that the basal levels of both Pi3,4P (Fig. 2 *A* and *B*) and Pi3,4,5P (Fig. S1 *A* and *B*) were increased in Aβ42-expressing neurons (*elav/Y;UAS-Aβ42/+*) compared with the controls (*elav/Y;+/+*). This increase is suppressed by application of wortmannin (Fig. 2 *A* and *B*). In contrast, insulin was capable of stimulating an increase in the targeted phospholipids in the controls, but it failed to further elevate them in Aβ42-expressing neurons (Fig. 2 *A* and *B* and Fig. S1 *A* and *B*). Thus, PI3K is indeed stimulated by Aβ42 expression.

Using different techniques, we have shown PI3K hyperactivity both at the NMJ and in the ventral ganglion, indicating that elevated PI3K activity may be a general feature of Aβ42 expression in neurons. It prompted our effort in testing if the observed PI3K hyperactivity contributed to the memory deficits observed in Aβ42-expressing adult fruit flies. With an extensively characterized Pavlovian olfactory aversive conditioning (*Methods*), our previous studies showed that 2-day-old Aβ42-expressing adult flies (*elav/Y;UAS-Aβ42/+*) have a normal immediate memory (7, 8), but a significant defect of this immediate memory occurs as early as 5 days (Fig. 3 *A* and *B*) and is also detectable in 10- and 15-day-old flies (Fig. S2). However, it is unsuitable to use flies older than 15 days for the memory assay, because these animals display Aβ42-induced locomotion defects (7). We chose 5-day-old flies for testing the effects of genetic manipulations, because the Aβ42-induced memory phenotype at this age was still in progression, making it is possible to observe both ameliorated and exacerbated memories in Aβ42-expressing flies. The Aβ42-induced age-dependent memory loss was prevented by knocking-down P60, the regulatory subunit of PI3K, through RNA interference (*elav/Y;UAS-Aβ42/+;UAS-dp60 RNAi/+*) (Fig. 3*A*). Additionally, a better memory was observed in 10- or even 15-day-old Aβ42-expressing flies with silenced PI3K function (Fig. S2). The significance of this observation was strengthened by the improved memory in Aβ42-expressing flies with overexpression of the phosphatase and tensin homolog (PTEN), a negative regulator of PI3K (*elav/Y;UAS-Aβ42/+;UAS-dpten/+*) (Fig. 3*B*). Conversely, Aβ42-induced memory loss was enhanced in 5-day-old female flies with an overexpression of a dominant negative mutant $PTEN^{C124S}$, which is a catalytically inactive form of PTEN (*elav/+;UAS-Aβ42/+;UAS-pten*^{C124S}*/+*) (Fig. 3*C*). Female flies were used in this particular experiment, because female Aβ42-expressing flies at this age showed a milder memory-loss phenotype compared with adult males because of the gene-dosage effect (7). Therefore, the enhanced memory loss was more easily revealed. Inhibition of PI3K with P60 RNAi or overexpressed PTEN alone had no significant effect on memory performance, although overexpression of $PTEN^{C124S}$ showed a mild but significant reduction in memory scores (Fig. S3 *A* and *B*). Flies of all genotypes showed normal sensorimotor ability (Table S1). Taken together, the Aβ42-induced memory loss can be rescued through inhibition of PI3K hyperactivity through genetic manipulations.

To exclude potential developmental effects associated with genetic manipulations of PI3K activity before eclosion, we

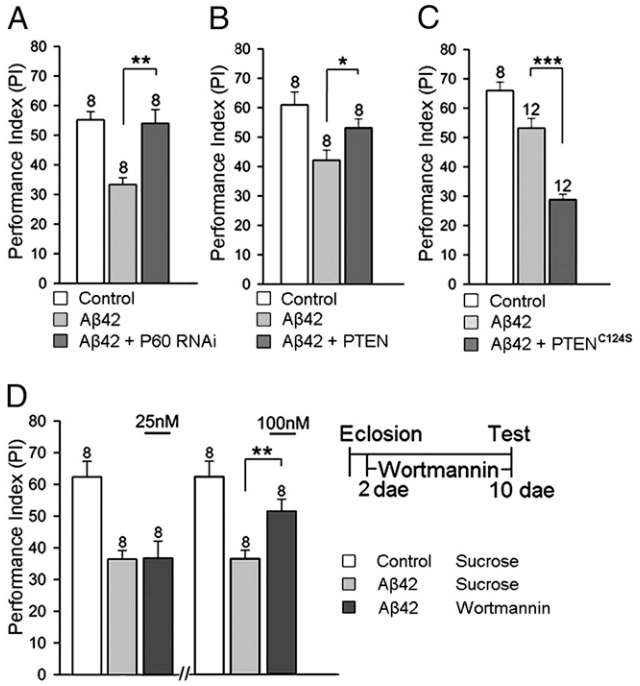

Fig. 3. Inhibition of PI3K activity ameliorates the Aβ42-induced immediate memory loss, whereas activation of PI3K activity causes an exacerbated memory defect. (*A* and *B*) Expression of Aβ42 in fly brains induced an immediate memory loss compared with control flies (*elav/Y;UAS-Aβ42/+* versus *+/Y;UAS-Aβ42/+*) at 5 days old. The immediate memory was ameliorated through inhibition of PI3K activity with P60 RNAi (*elav/Y;UAS-Aβ42/+; UAS-dp60 RNAi/+*) (*A*, *t* test; $^{**}P < 0.01$) or overexpression of PTEN, a negative regulator of PI3K pathway (*elav/Y;UAS-Aβ42/+;UAS-dpten/+*) (*B*, *t* test; $^{*}P < 0.05$). Overexpression of the dominant negative $PTEN^{C124S}$ in female flies exacerbated the Aβ42-induced memory loss at 5 days old. (*elav/+;UAS-Aβ42/+* versus *elav/+;UAS-Aβ42/+;UAS-pten^{C124S}/+*; *C*, *t* test; $^{***}P < 0.001$). (*D Left*) Control flies were fed with sucrose, whereas Aβ42-expressing flies were fed with sucrose or wortmannin. The Aβ42-induced memory loss was ameliorated by treatment of 100 nM wortmannin (*t* test; $^{**}P < 0.01$) but not 25 nM wortmannin. (*Right*) Drug treatment started 2 days after eclosion (dae), and the immediate memory was tested at 10 dae. Data are expressed as means ± SEM (n = 8-12 PIs as indicated).

looked at effects of a pharmacological treatment of wortmannin, the PI3K inhibitor, on adult male flies. Two drug-feeding paradigms were tested. For the first paradigm, drug feeding began with 2-day-old flies, before any observable behavioral defects, for 4 h each day for 7 consecutive days. The memory scores were determined on day 10 (Fig. 3*D Right*). Improved memory was seen in Aβ42-expressing flies with 100 nM, but not 25 nM, drug treatment (Fig. 3*D Left*). This result was confirmed with another PI3K inhibitor, LY294002 (Fig. S4).

The second drug feeding (wortmannin, 100 nM) test began at day 5 after eclosion when memory was significantly lower in Aβ42-expressing flies (Fig. 3 *A* and *B*), and it continued for 7 days. Then, memory was assayed on day 13 (Fig. S5*A Upper*). Memory was significantly better in Aβ42-expressing flies with the drug treatment compared with those treated with sucrose (Fig. S5*A*). Both paradigms of the drug treatment used in this study did not influence the sensorimotor ability of Aβ42-expressing flies (Table S2). The rescuing effect confirmed that the Aβ42-induced memory loss resulted from an elevated PI3K activity.

To gain insights into how PI3K contributes to Aβ42-induced phenotypes, we evaluated accumulation of Aβ42 aggregates. Aβ peptides accumulate in different forms, including monomer, oligomers, and fibrils. Aβ oligomers have recently come into focus as the major pathological species of Aβ peptides, and they can cause learning defects in mice (3, 21, 22). To determine the oligomer level, whole-head lyses were used for the Western blot assay. For stronger signals, 15-day-old male flies were chosen (older flies have higher levels of accumulated Aβ42). Here, we found that the ratio of oligomers (dimmers and trimmers; see bands pointed by two arrows in Fig. 4 *Left*) to monomer (pointed by the arrow head in Fig. 4) was significantly lower in Aβ42-expressing flies with inhibition of PI3K activity through either knocking-down P60 or overexpression of PTEN (Fig. 4). Note that the Aβ42 monomer level was not affected (Fig. S6). However, we must point out that the reduction in the oligomer level was moderate. A similar level of reduction was also observed in 13-day-old Aβ42-expressing flies after the drug (wortmannin) treatment (Fig. S5*B*).

Thioflavin-S (TS) staining of the whole brain was used to specifically visualize the Aβ42 fibril deposits (Fig. 5*A*) (8, 23). This analysis was performed in two different age groups: 15-day-old flies, at which immediate memory and accumulation of oligomers were measured, and 50-day-old flies, at which extensive neurodegeneration has been reported (8). Our examination focused on the mushroom-body (MB) region, because it is easily identified anatomically and is considered to be a neural center for olfactory associative-memory formation in fruit flies.

In contrast to the fairly moderate reduction in oligomer levels, we were surprised to see that fibril Aβ42 deposits were dramatically reduced by inhibition of PI3K activity. We classified the deposits into three categories on basis of size: 1–1.5 μm, 1.5–2 μm, and >2 μm in diameter. The deposits grew larger in size with age. Inhibition of PI3K activity through knocking down the P60 subunit in *elav/Y;UAS-Aβ42/+;UAS-dp60 RNAi/+* transgenic flies led to a drastic reduction in the number of deposits. For younger flies, the reduction occurred in the smaller deposits, whereas for older flies, the reduction was mainly on the larger deposits (Fig. 5 *A* and *B*). Such a reduction was also observed in 13-day-old Aβ42-expressing flies after drug feeding with 100 nM wortmannin for 7 days (Fig. S5*C*).

We were intrigued by such a dramatic effect. In particular, fibril deposits have been suggested to be critical in neurodegeneration (24). Severe degeneration was evident in TS-staining images of 50-day-old male flies with or without knocking down the P60 subunit (the black holes in Fig. 5*A Lower*). Then, we performed H&E staining of the female brain slices at 40 days of age hoping to more easily detect an improvement when the degeneration was milder. We quantified the ratio of the degenerative areas within the MB somatic region and used it to indicate the severity of degeneration (8). There was no difference observed between Aβ42-expressing flies with or without silenced PI3K (Fig. 6).

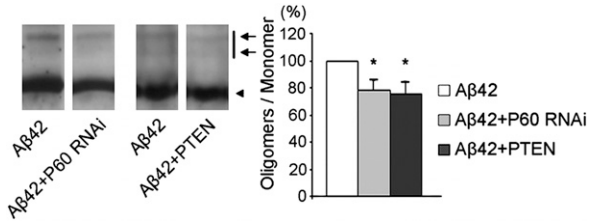

Fig. 4. Inhibition of PI3K activity reduces the accumulation of Aβ42 oligomers. (*Left*) Aβ42 oligomer levels of indicated genotypes were detected by Western blot with whole-head lyses of 15-day-old flies. Arrows indicate oligomer bands. Arrowhead indicates monomer band. (*Right*) Oligomers to monomer ratios were calculated and normalized to Aβ42-expressing heads (*elav/Y;UAS-Aβ42/+*). Aβ42 oligomer levels were reduced in fly heads with inhibited PI3K activity by either P60 RNAi or overexpressed PTEN (*elav/Y;UAS-Aβ42/+;UAS-dp60 RNAi/+* or *elav/Y;UAS-Aβ42/+;UAS-dpten/+*; *t* test; $^{*}P < 0.05$). Data are expressed as means ± SEM (n = 3 independent experiments for each genotype).

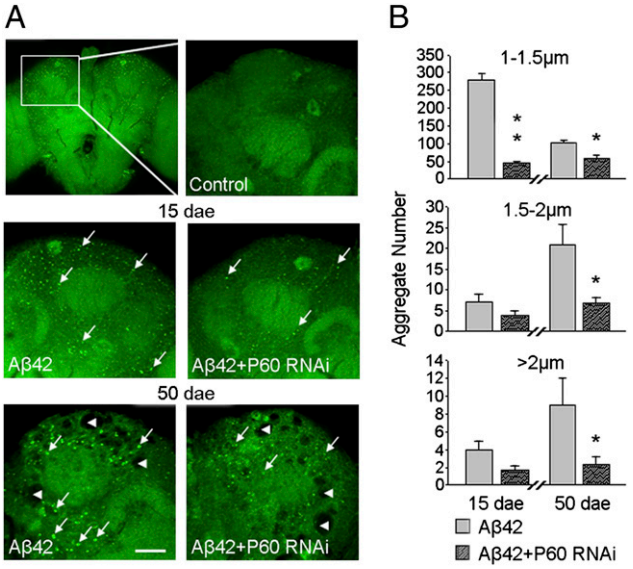

Fig. 5. Reduced PI3K activity decreases Aβ42 fibril deposits. (*A*) TS staining was used to detect the Aβ42 fibril deposits in the fly brains. No deposits were found in control brains (*elav/Y;+/+*; *Top Right*) at 15 dae. TS-positive deposits (arrow) were found after Aβ42 expression in fly brains (*elav/Y;UAS-Aβ42/+*) at both 15 dae (*Middle Left*) and 50 dae (*Bottom Left*). Neurodegeneration in the brain was also been detected at 50 dae (arrowhead). (*B*) Deposits were classified by the size into three groups: 1–1.5 μm, 1.5–2 μm, and >2 μm. Genetic inhibition of PI3K by P60 RNAi (*elav/Y;UAS-Aβ42/+;UAS-dp60 RNAi/+*) could reduce the deposit quantities of all of the three groups, especially at 50 dae (*t* test; $*P < 0.05$; $**P < 0.01$). Data are expressed as means ± SEM ($n = 4$ and 3 brains for 15 dae and 50 dae flies, respectively). (Scale bar, 25 μm.)

Thus, although inhibition of PI3K rescued early memory loss, it had no effect on Aβ42-induced neurodegeneration.

Discussion

The goal of this study is to identify biochemical pathways through which Aβ42 induces age-dependent memory loss. We began by studying LTD at the larval NMJ, because this preparation is suitable for rapid testing of pharmacological and genetic manipulations. It indeed provided a clue of PI3K hyperactivity. We then moved to the ventral ganglion preparation that is suitable for quantifying immunoreactivity of phospholipids. A positive result of this study suggested that PI3K hyperactivity might be a general feature of Aβ42 effects. We went on to show that inhibition of PI3K activity could rescue Aβ42-induced memory loss. This behavioral effect is correlated with a mild reduction in the accumulation of Aβ42 oligomers as well as a strong reduction in Aβ42 fibril deposits.

The PI3K/Akt pathway has attracted attention for its pivotal role in regulating cell survival, proliferation, and synaptic transmission (25). Although several works have been reported in studying its role in Aβ toxicity, the conclusions remained controversial. In vitro studies show that application of Aβ42 reduced Akt activity, and consequently, elevated Akt activity is capable of reducing Aβ42-induced cell death in culture (26). However, another study showed that acute exposure of primary mouse neurons to Aβ42 up-regulated Akt phosphorylation (27). More importantly, an increase in Akt activity was found in the temporal cortex of the postmortem AD brain, suggesting an up-regulated PI3K/Akt pathway in patients (28–30). Consistent with the postmortem study, our in vivo analysis revealed that accumulation of Aβ42 seemed to increase PI3K activity at the larval NMJ, larval ganglion neurons, and the adult brain. This enhanced activity was responsible for altered LTD, an abnormal insulin response, and the age-dependent memory loss.

It is interesting to note that in patients, AD has been notoriously known as brain diabetes, because the brain tissue is shown to be insulin resistant (31, 32). As indicated in this study, Aβ42-stimulated PI3K can be an explanation of such resistance. The basal level of PI3K was elevated to a level by an overloading of Aβ42 so that insulin was unable to further stimulate its activity. We speculate that restoring the dynamic range for PI3K activity, but not simply inhibiting PI3K activity, could be responsible for the rescued immediate memory.

In association with the rescued memory loss, we found a mild reduction in accumulation of Aβ42 oligomers and a drastic decrease in fibril deposits. Interestingly, oral administration of PI3K inhibitor also reduced the Aβ accumulation in mice (33). This is consistent with reports that accumulation of Aβ oligomers is associated with memory loss in mouse AD models, and injection of Aβ dimers purified from AD patient brains into rat brain can cause memory loss (2, 3, 22). It would be of interest to see if the reduced fibril deposits also contributed to the improved memory.

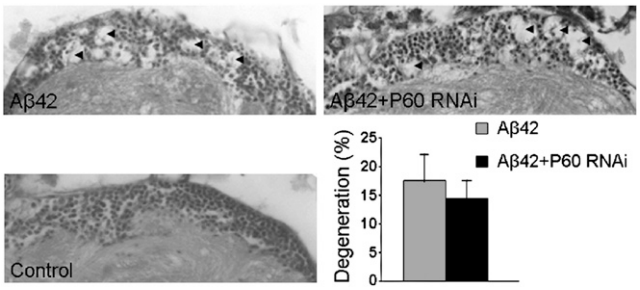

Fig. 6. Aβ42-induced neurodegeneration is not rescued by attenuation of PI3K activity. Paraffin slices were taken from 40-day-old female flies and then, were stained with H&E. The MB somatic region is used to quantify the severity of degeneration by calculating the ratio of degenerative area to total area (histogram). Control flies (*elav/+;+/+*) had entire cell-body region at this age. Expression of Aβ42 in fly brains induced neurodegeneration (arrowhead) that was not recovered by inhibiting PI3K activity with P60 RNAi (*elav/+;UAS-Aβ42/+* versus *elav/+;UAS-Aβ42/+;UAS-dp60 RNAi/+*; *t* test; $P > 0.05$). Data are expressed as means ± SEM ($n = 6$ brains for each genotype).

Materials and Methods

***Drosophila* Genetics and Stocks.** Transgenic fly lines used in this report have been previously described, including *UAS-Aβ42* (8, 13), *elav ^{C155}-Gal4*, *G7-Gal4* (34), *UAS-dpten* (35), and *UAS-pten ^{C124S}* (36). The *UAS-p60 RNAi* was obtained from the Vienna *Drosophila* RNAi Center. Flies were raised and maintained at room temperature (22–24 °C). All stocks used for Pavlovian olfactory conditioning were equilibrated by five generations of out-cross to *w^{1118}* (*isoCJ1*).

Electrophysiology. Two-electrode voltage-clamp electrophysiological recordings were performed as described previously (17). In brief, wall-climbing third-instar larvae were chosen for dissection. Larvae were dissected at room temperature and in Ca^{2+}-free hemolymph-like (HL-3.1) solution (37) containing the following: 70 mM NaCl, 5 mM KCl, 4 mM $MgCl_2$, 10 mM $NaHCO_3$, 5 mM trehalose, 5 mM Hepes, and 115 mM sucrose. All recordings were made at the longitudinal muscles of segments A4–A5 and muscle fiber 12 with 0.4 mM $CaCl_2$. The segmental nerve was stimulated at 1.5 times the stimulus voltage required for a threshold response for Excitatory Junction Currents (EJCs). For recordings of LTD, the nerve was stimulated at a baseline frequency of 0.05 Hz for 5 minutes and 30 Hz for induction of LTD. Current signals were amplified with an Axoclamp 2B amplifier (Molecular Devices). The signals were digitized using a Digidata 1320A interface (Molecular Devices) and acquired by pClamp 9.0 software (Molecular Devices). To minimize variation, each experimental group was only compared with a dedicated control group with a similar genetic background and was recorded in the same batch of experiments. Evoked responses were analyzed using the Mini Analysis Program (Synaptosoft).

Lipid Analysis. Wall-climbing third-instar larvae were used for dissection. Larvae were dissected at room temperature and in Ca^{2+}-free HL-3.1 solution. After incubation with 1.7 μM bovine insulin (Sigma) or 100 nM wortmannin (Sigma) for 30 minutes, animals were fixed with 4% paraformaldehyde (Electron Microscopy Sciences) for 20 minutes and then changed to 0.5% spatonin for 20 minutes. Samples were blocked with normal goat serum (Jackson Immunoresearch Laboratories), incubated with mouse anti-PI3,4P or mouse anti-PI3,4,5P antibodies (Echelon Biosciences) and then inspected with the Zeiss LSM 510 confocal system. Five different cells from each genotype were chosen for comparison by calculating the fluorescence ratio of the peripheral region to the central region. LSM 510 analysis software (Zeiss) was used.

Pavlovian Olfactory Associative Immediate Memory. The training and testing procedures were the same as previously described (38). During one training session, a group of 100 flies was sequentially exposed for 60 seconds to two odors, 3-octanol (OCT; Fluka) or 4-methylcyclohexanol (MCH; Fluka), with 45 seconds of fresh air in between the exposure. Flies were subjected to foot shock (1.5-second pulses with 3.5-second intervals; 60 V) during exposure to the first odor (CS+) but not during exposure to the second odor (CS−). To measure immediate memory (also referred to as learning), flies were transferred immediately after training to the choice point of a T-maze and were forced to choose between the two odors for 2 minutes. Then, flies were trapped in their respective T-maze arms, anesthetized, and counted. A performance index (PI) was calculated from the distribution of this group of flies in the T-maze. A reciprocal group of flies was trained and tested by using OCT as the CS+ and MCH as the CS+, respectively. The so-called half-PIs (OCT) and PI (MCH) were finally averaged for an $n = 1$ and multiplied by 100. A PI of 0 indicated a distribution of 50:50 (no learning), whereas a PI of 100 indicated perfect learning (100% of the flies avoided the CS+ previously paired with foot shock). Control groups are age-matched to the experimental groups in each test.

Sensorimotor Responses. Odor-avoidance (OA) responses were quantified by exposing naïve flies to one odor (OCT or MCH) versus air in the T-maze (38). After 2 minutes, flies were trapped in their respective T-maze arms, anesthetized, and counted. A PI was calculated for each odor individually as reported (38). The ability to sense and escape from foot shock [shock reactivity (SR)] was quantified in naïve flies by inserting electrifiable grids into both arms of the T-maze and delivering shock pulses only in one arm of the T-maze, allowing flies to choose between the two arms. After 2 minutes, flies were trapped in their respective arms, anesthetized, and counted. Individual PIs were calculated as for olfactory acuity.

Drug-Feeding Treatment. Wortmannin and LY294002 (Sigma) were dissolved in DMSO (Sigma) and stored at −20 °C. Flies were starved for 3 hours in empty vials and then fed with drugs, diluted in 4% sucrose, for another 4 hours. Flies were transferred to normal food after treatment. Drug feeding was carried out one time each day during the treatment period. The final concentrations used were 25 nM/50 nM/100 nM for wortmannin and 30 μM for LY294002.

Fibril Aβ42 Deposits Detection. TS (Sigma) staining was performed to detect fibril Aβ42 deposits as described previously (8, 23). Fly brains were fixed in 4% paraformaldehyde and permeabilized by 2% triton. Brains were then transferred to 0.25% TS in 50% ethanol for 1 night and destained for 10 minutes in 50% ethanol. After three washes with PBS, they were mounted using focusclear (Pacgen Biopharmaceuticals Inc.), and coverslips were added. Slides were inspected with a Zeiss LSM 510 confocal microscope. LSM 510 analysis software was used.

Western Blot Analysis. Whole-head lyses were diluted in SDS sample buffer, separated by 10–20% Tris-Tricine gels (Invitrogen), and transferred to nitrocellulose membranes (Invitrogen). The membranes were boiled in PBS for 3 minutes, blocked with 5% nonfat dry milk, and blotted with the 6E10 antibody (Covance Research Products). Data were analyzed with software ImageJ (National Institutes of Health).

Quantification of Neurodegeneration. Heads were fixed in 4% paraformaldehyde, processed to embed in paraffin blocks, and sectioned at a thickness of 6 μm. Sections were placed on slides, stained with H&E (Vector), and examined by bright-field microscopy. The area of the vacuoles in the mushroom-body cell-body region was measured in each image with software ImageJ. The ratio was calculated by dividing the sum of the vacuole areas by the total area of the cell-body region.

Statistical Analysis. All data were analyzed by using Student *t* tests (SigmaPlot version 10.0; Systat Software Inc.). Statistical results are presented as means ± SEM. Asterisks indicate critical values ($*P < 0.05$; $**P < 0.01$, and $***P < 0.001$).

ACKNOWLEDGMENTS. We thank Dr. Bruce Edgar, Dr. Tian Xu, Bloomington Stock Center, and Vienna *Drosophila* RNAi Center for providing transgenic flies, JoeKai, Inc. for technical support, and Dr. Jennifer Beshel and Dr. Robert Campbell for constructive comments on the manuscript. This work was supported by Grant 2R01 NS34779-06 from the US National Institutes of Health (to Y.Z.), Grant DAMD17-99-1-9500 from the US Army Neurofibromatosis Research Program (to Y.Z.), Dart Neuroscience, Grant 2009CB941301 from the National Basic Research Project (973 program) of the Ministry of Science and Technology of China (to Y.Z.), and the Tsinghua-Yue-Yuen Medical Sciences Fund (Y.Z.).

1. Tanzi RE, Bertram L (2005) Twenty years of the Alzheimer's disease amyloid hypothesis: A genetic perspective. *Cell* 120:545–555.
2. Walsh DM, et al. (2002) Naturally secreted oligomers of amyloid beta protein potently inhibit hippocampal long-term potentiation in vivo. *Nature* 416:535–539.
3. Haass C, Selkoe DJ (2007) Soluble protein oligomers in neurodegeneration: Lessons from the Alzheimer's amyloid beta-peptide. *Nat Rev Mol Cell Biol* 8:101–112.
4. Small DH, Mok SS, Bornstein JC (2001) Alzheimer's disease and Abeta toxicity: From top to bottom. *Nat Rev Neurosci* 2:595–598.
5. Pereira C, Agostinho P, Moreira PI, Cardoso SM, Oliveira CR (2005) Alzheimer's disease-associated neurotoxic mechanisms and neuroprotective strategies. *Curr Drug Targets CNS Neurol Disord* 4:383–403.
6. Götz J, Ittner LM (2008) Animal models of Alzheimer's disease and frontotemporal dementia. *Nat Rev Neurosci* 9:532–544.
7. Iijima K, et al. (2004) Dissecting the pathological effects of human Abeta40 and Abeta42 in Drosophila: A potential model for Alzheimer's disease. *Proc Natl Acad Sci USA* 101:6623–6628.
8. Iijima K, et al. (2008) Abeta42 mutants with different aggregation profiles induce distinct pathologies in Drosophila. *PLoS One* 3:e1703.
9. Torroja L, Packard M, Gorczyca M, White K, Budnik V (1999) The *Drosophila* beta-amyloid precursor protein homolog promotes synapse differentiation at the neuromuscular junction. *J Neurosci* 19:7793–7803.
10. Li Y, Liu T, Peng Y, Yuan C, Guo A (2004) Specific functions of *Drosophila* amyloid precursor-like protein in the development of nervous system and nonneural tissues. *J Neurobiol* 61:343–358.
11. Carmine-Simmen K, et al. (2009) Neurotoxic effects induced by the *Drosophila* amyloid-beta peptide suggest a conserved toxic function. *Neurobiol Dis* 33:274–281.
12. Luo L, Tully T, White K (1992) Human amyloid precursor protein ameliorates behavioral deficit of flies deleted for Appl gene. *Neuron* 9:595–605.
13. Chiang HC, Iijima K, Hakker I, Zhong Y (2009) Distinctive roles of different β-amyloid 42 aggregates in modulation of synaptic functions. *FASEB J* 23:1969–1977.
14. Keshishian H, Broadie K, Chiba A, Bate M (1996) The *drosophila* neuromuscular junction: A model system for studying synaptic development and function. *Annu Rev Neurosci* 19:545–575.
15. Jan LY, Jan YN (1976) Properties of the larval neuromuscular junction in *Drosophila melanogaster*. *J Physiol* 262:189–214.
16. Zhong Y, Wu CF (1991) Altered synaptic plasticity in *Drosophila* memory mutants with a defective cyclic AMP cascade. *Science* 251:198–201.
17. Guo HF, Zhong Y (2006) Requirement of Akt to mediate long-term synaptic depression in *Drosophila*. *J Neurosci* 26:4004–4014.
18. Hannan F, et al. (2006) Effect of neurofibromatosis type I mutations on a novel pathway for adenylyl cyclase activation requiring neurofibromin and Ras. *Hum Mol Genet* 15:1087–1098.
19. de Marco A, Cozzi R (1980) Chromosomal aberrations induced by caffeine in somatic ganglia of *Drosophila melanogaster*. *Mutat Res* 69:55–69.
20. Gorczyca M, Augart C, Budnik V (1993) Insulin-like receptor and insulin-like pep>tide are localized at neuromuscular junctions in *Drosophila*. *J Neurosci* 13:3692–3704.
21. Lesné S, et al. (2006) A specific amyloid-beta protein assembly in the brain impairs memory. *Nature* 440:352–357.
22. Shankar GM, et al. (2008) Amyloid-beta protein dimers isolated directly from Alzheimer's brains impair synaptic plasticity and memory. *Nat Med* 14:837–842.
23. Fay DS, Fluet A, Johnson CJ, Link CD (1998) In vivo aggregation of β-amyloid peptide variants. *J Neurochem* 71:1616–1625.
24. Urbanc B, et al. (2002) Neurotoxic effects of thioflavin S-positive amyloid deposits in transgenic mice and Alzheimer's disease. *Proc Natl Acad Sci USA* 99:13990–13995.
25. Franke TF (2008) PI3K/Akt: Getting it right matters. *Oncogene* 27:6473–6488.
26. Ma R, et al. (2009) Erythropoietin protects PC12 cells from beta-amyloid(25-35)-induced apoptosis via PI3K/Akt signaling pathway. *Neuropharmacology* 56:1027–1034.
27. Abbott JJ, Howlett DR, Francis PT, Williams RJ (2008) Abeta(1-42) modulation of Akt phosphorylation via alpha7 nAChR and NMDA receptors. *Neurobiol Aging* 29:992–1001.
28. Rickle A, et al. (2006) PTEN levels in Alzheimer's disease medial temporal cortex. *Neurochem Int* 48:114–123.

29. Nakagami Y (2004) Inhibitors beta-amyloid-induced toxicity by modulating the Akt signaling pathway. *Drug News Perspect* 17:655–660.
30. Rickle A, et al. (2004) Akt activity in Alzheimer's disease and other neurodegenerative disorders. *Neuroreport* 15:955–959.
31. Craft S, et al. (1998) Cerebrospinal fluid and plasma insulin levels in Alzheimer's disease: Relationship to severity of dementia and apolipoprotein E genotype. *Neurology* 50:164–168.
32. Zhao WQ, Townsend M (2009) Insulin resistance and amyloidogenesis as common molecular foundation for type 2 diabetes and Alzheimer's disease. *Biochim Biophys Acta* 1792:482–496.
33. Haugabook SJ, et al. (2001) Reduction of Abeta accumulation in the Tg2576 animal model of Alzheimer's disease after oral administration of the phosphatidyl-inositol kinase inhibitor wortmannin. *FASEB J* 15:16–18.
34. Renden RB, Broadie K (2003) Mutation and activation of Galpha s similarly alters pre- and postsynaptic mechanisms modulating neurotransmission. *J Neurophysiol* 89: 2620–2638.
35. Britton JS, Lockwood WK, Li L, Cohen SM, Edgar BA (2002) *Drosophila*'s insulin/PI3-kinase pathway coordinates cellular metabolism with nutritional conditions. *Dev Cell* 2:239–249.
36. Huang H, et al. (1999) PTEN affects cell size, cell proliferation and apoptosis during *Drosophila* eye development. *Development* 126:5365–5372.
37. Feng Y, Ueda A, Wu CF (2004) A modified minimal hemolymph-like solution, HL3.1, for physiological recordings at the neuromuscular junctions of normal and mutant *Drosophila* larvae. *J Neurogenet* 18:377–402.
38. Tully T, Quinn WG (1985) Classical conditioning and retention in normal and mutant *Drosophila melanogaster*. *J Comp Physiol [A]* 157:263–277.